Original Paper

Brain, Behavior and Evolution

Brain Behav Evol 2017;90:62–72
DOI: 10.1159/000475591

Published online: September 4, 2017

Functional Connectivity Pattern of the Internal Hippocampal Network in Awake Pigeons: A Resting-State fMRI Study

Mehdi Behroozi[a] Felix Ströckens[a] Martin Stacho[a] Onur Güntürkün[a, b]

[a]Department of Biopsychology, Institute of Cognitive Neuroscience, Faculty of Psychology, Ruhr University Bochum, Bochum, Germany; [b]Stellenbosch Institute for Advanced Study (STIAS)/Wallenberg Research Centre at Stellenbosch University, Stellenbosch, South Africa

Keywords
Avian hippocampus · Magnetic resonance imaging · Hippocampal connectivity · Navigation

Abstract
In the last two decades, the avian hippocampus has been repeatedly studied with respect to its architecture, neurochemistry, and connectivity pattern. We review these insights and conclude that we unfortunately still lack proper knowledge on the interaction between the different hippocampal subregions. To fill this gap, we need information on the functional connectivity pattern of the hippocampal network. These data could complement our structural connectivity knowledge. To this end, we conducted a resting-state fMRI experiment in awake pigeons in a 7-T MR scanner. A voxel-wise regression analysis of blood oxygenation level-dependent (BOLD) fluctuations was performed in 6 distinct areas, dorsomedial (DM), dorsolateral (DL), triangular shaped (Tr), dorsolateral corticoid (CDL), temporo-parieto-occipital (TPO), and lateral septum regions (SL), to establish a functional connectivity map of the avian hippocampal network. Our study reveals that the system of connectivities between CDL, DL, DM, and Tr is the functional backbone of the pigeon hippocampal system. Within this network, DM is the central hub and is strongly associated with DL and CDL BOLD signal fluctuations. DM is also the only hippocampal region to which large Tr areas are functionally connected. In contrast to published tracing data, TPO and SL are only weakly integrated in this network. In summary, our findings uncovered a structurally otherwise invisible architecture of the avian hippocampal formation by revealing the dynamic blueprints of this network.

Introduction

All vertebrates have to orient in space, and all of them seem to rely on hippocampal circuits to do so [Treves et al., 2008]. In amniotes, the hippocampal area derives from the medial pallium during embryonic development, and, accordingly, the dorsomedial hippocampal pallium in reptiles, mammals, and birds is considered to be homologous [Bingman et al., 2009; Herold et al., 2015]. This pallial entity probably possessed a trilaminar organization of its ancestral amniote form and then underwent different changes in mammalian and avian lineages [Striedter, 2016]. Thus, hippocampal functions seem to be conserved through hundreds of millions of years of

KARGER

E-Mail karger@karger.com
www.karger.com/bbe

Onur Güntürkün
Department of Biopsychology, Institute of Cognitive Neuroscience
Faculty of Psychology, Ruhr University Bochum
Universitätsstrasse 150, DE–44780 Bochum (Germany)
E-Mail onur.guentuerkuen@rub.de

divergent evolution, despite radical differences in the overall architecture of the hippocampal area. To understand this apparent discrepancy, we have to analyze the function and the architecture of hippocampal areas of different vertebrate lineages in greater detail to identify its shared and nonshared blueprints. This paper describes a novel approach in this pursuit by analyzing the functional connectivity of the intrahippocampal network and its closely associated structures in pigeons using high magnetic field imaging techniques.

In mammals, the three-layered hippocampus can be roughly subdivided into the dentate gyrus and the cornu ammonis (Ammon's horn). The dentate gyrus is mainly characterized by a prominent granule cell layer that receives input from the entorhinal cortex via the perforant pathway and projects via its mossy fibers to Ammon's horn. Ammon's horn contains a pyramidal cell layer and can be separated into four subregions (CA1–4). Especially in CA3, the pyramidal neurons give rise to extensive collaterals forming a recurrent connectivity network [Herold et al., 2015]. Despite similar functions, the avian hippocampal formation is structured quite differently. It seems to have lost a clear trilaminar appearance and lacks overall granule and pyramidal cell layers [Tömböl et al., 2000a, b; Herold et al., 2015]. The avian hippocampal formation, is, however, not a simplified version of the mammalian one but has developed a different internal architecture that we outline in the following.

Based on studies analyzing cytoarchitecture, neuropeptide expression, and receptor densities, different authors proposed slightly different subdivisions of the avian hippocampal system [Erichsen et al., 1991; Kahn et al., 2003; Herold et al., 2014; Atoji et al., 2016]. The most recent study of Herold et al. [2014; see also Smulders, 2017] in pigeons distinguished four major subdivisions by autoradiographically mapping the distribution of 11 neurotransmitter receptors and combining these data with an analysis of the staining for the heavy metal zinc. Moving from lateral to medioventral, the first entity is the dorsolateral region (DL) that can be subdivided into a dorsal component with dense kainate receptors and a ventral division that expresses 5-HT1A receptors. The next area is the dorsomedial region (DM) that can be subdivided into a zinc-free dorsal area and a ventral component that is characterized by a moderate zinc density. DL and DM are mostly identical to the area parahippocampalis (APH) of older avian hippocampus studies [Karten and Hodos, 1967]. The ventral hippocampus is constituted by a V-shaped complex (V) that consists of two narrow wings that encapsulate the triangular region (Tr). This area contains pyramidal-like neurons that seem to be arranged like the mammalian CA3 field and could constitute an auto-associative system for memory completion [Tömböl et al., 2000a, b; Treves et al., 2008]. Based on details of these subdivisions, Herold et al. [2014] concluded that the avian hippocampal subdivisions only resemble parts of the mammalian Ammons's horn or dentate gyrus, making it likely that the independent evolutionary paths of mammals and birds led to "a mosaic of similarities and differences" in their hippocampal formations.

In a large-scaled tracing study, Atoji and Wild [2004] analyzed the connections of the pigeon's hippocampal formation and discovered that the intrahippocampal circuitry was strongly and reciprocally interconnected [Hough et al., 2002; Kahn et al., 2003]. These studies led to the suggestion that the pathway running from DL to DM, from DM to V, and from V back to DM constitutes the major feedforward network of the avian hippocampus [Hough et al., 2002; Kahn et al., 2003; Bingman et al., 2005]. In addition, both DL and DM receive afferents from numerous areas and seem to serve as major input regions into the hippocampal formation. Sensory information about visual and olfactory senses is funneled via the CDL (area corticoidea dorsolateralis) to all main hippocampal subregions [Atoji and Wild, 2004, 2005; Patzke et al., 2011; Atoji and Wild, 2014]. Furthermore, DL and DM also serve as the main hippocampal output areas and project to various telencephalic and diencephalic structures, with most of these projections being reciprocal [Atoji and Wild, 2004]. Interestingly, the lateral septum (SL) receives input from DM but neither SL nor medial septum have strong back projections [Atoji and Wild, 2004; Atoji et al., 2016]. The lack of strong reciprocal connectivity is an important difference to the mammalian hippocampus where the medial septum has a strong cholinergic and glutamatergic back projections to the hippocampus that drive hippocampal theta rhythms, thereby facilitating learning and memory [Winson, 1978; Leutgeb and Mizumori, 1999; Strange et al., 2014; Vandecasteele et al., 2014; Herold et al., 2015; Robinson et al., 2016]. A further critical area is the TPO (area temporo-parieto-occipitalis) that has reciprocal connections with the CDL and is also connected to CDL via the dorsal thalamus [Atoji and Wild, 2005]. The pigeon connectome [Shanahan et al., 2013] reveals that the TPO integrates multimodal information and could funnel sensory input via the CDL into the hippocampal system.

This short overview of the main subdivisions and connectivity patterns shows the similarities and differences between the avian and the mammalian hippocampal for-

mation. To further this comparison and to better understand the avian hippocampus, we need to combine function with structural and connectional data. This is possible by using recently developed resting-state functional connectivity techniques in functional magnetic resonance imaging (rs-fMRI) [Fox and Raichle, 2007; Di Martino et al., 2008; Kaplan et al., 2016]. Such studies have been proven to be powerful tools to investigate the functional coupling between different brain regions in humans, monkeys, and rodents [Logothetis et al., 2001; van den Heuvel and Hulshoff Pol, 2010; Daliri and Behroozi, 2014; Kaplan et al., 2016]. The rationale behind these experiments is the following: Brain areas that interact with each other often synchronize their neural activity patterns, both with respect to fast and slow fluctuations. This is visible in the ongoing changes in the blood oxygenation level-dependent (BOLD) signal of two studied brain areas of a resting animal. High correlations indicate a high level of neuronal coupling, while zero correlations indicate that these two areas fluctuate completely independently [Fox and Raichle, 2007; Di Martino et al., 2008]. Until today, only few studies have analyzed the functional connectivity of specific areas in the avian brain [De Groof et al., 2013; Jonckers et al., 2015]. To analyze the functional network of the hippocampal formation in pigeons, we conducted a study using rs-fMRI by focusing on the left and right hippocampal or hippocampus-associated regions Tr, DM, DL, CDL, SL, and TPO in order to examine possible functional connections between these areas.

Materials and Methods

Eight Valencian Figurita breed adult pigeons (*Columba livia*) were housed individually with a 12-h light:12-h dark cycle and water and food ad libitum. All procedures were carried out in accordance with the guidelines for the care and use of animals of the State of North Rhine-Westphalia in Germany. To control for motion artifacts by head movements, animals were implanted under anesthesia with an MR-compatible plastic pedestal for head fixation. Following surgery, analgesic and antibiotic treatment was administered for at least 3 days.

Before MR scanning, animals were habituated to the head holding device in a mock scanner by positioning the animals in a custom-made MR-compatible restrainer for increasing periods of time over 5 days (15, 30, and 60 min per day). After initial habituation, pigeons were fixated via their implanted plastic pedestal to the restrainer. The restrainer was placed in a mock scanner with an inner diameter of 8 cm. Animals were allowed a maximum of 10 days to acclimatize to the head holding condition. The length of fixation started from 10 min on the first day and was continually prolonged every day (10, 20, 40, and 60 min per day) until animals were habituated to the head fixation and showed no longer a visible stress response. In the last step of habituation, pigeons were acclimatized to the MR scanner sound [Hurwitz et al., 1989]. We recorded the scanner sound from various imaging sessions and played this sound for 60 min at a sound level of 50 dB, which increased by 10-dB steps per day until a sound level of 80 dB was reached.

MR Data Acquisition

All MRI measurements were conducted in a 7-T horizontal-bore small-animal scanner (Bruker BioSpec, 70/30 USR, Germany) using an 80-mm transmit quadrature birdcage resonator. A planar single-loop 20-mm coil for the acquisition of radio frequency pulses was positioned around the head to reduce motion artifacts resulting from body movements. MR images were acquired using the Bruker ParaVision 5.1 software. During MR scanning, the respiration rate was monitored using a respiration sensor.

At the start of the scanning session, three scans were acquired using a RARE sequence with the following imaging parameters: TR = 4 s, effective TE = 40.37 ms, RARE factor = 8, no average, acquisition matrix = 256 × 128, field of view (FOV) = 32 × 32 mm^2, spatial resolution = 0.125 × 0.25 mm, slice thickness = 1 mm, number of slices = 20 axial, 17 sagittal, and 15 coronal. Based on these images, the location of slices was determined and a slice package consisting of 11 coronal slices with no gap between slices was positioned in a way that the whole telencephalon was covered. Anatomical images of these slices were acquired using a RARE sequence with the following parameters: TR = 2 s, TE = 43.59 ms, RARE factor = 8, FOV = 30 × 30 mm^2, acquisition matrix = 128 × 128, and spatial resolution = 0.234 × 0.234 mm^2. Images were later used to register individual functional data to the previously obtained high-resolution anatomical images.

Based on the geometry of the anatomical images, resting-state data at each slice position were acquired using a single-shot multislice RARE sequence: TR = 2 s, TE = 33.7 ms, partial Fourier transform accelerator = 1.65, FOV = 30 × 30 mm^2, acquisition matrix = 64 × 64, spatial resolution = 0.47 × 0.47 mm^2, flip angle = 180°, slice thickness = 1 mm, no interslice distance, slice order = interleaved. Each run included 300 volumes, with the first 10 volumes being used to compensate for T1 saturation artifacts. A total of 23 scans (300 volumes per sessions) were acquired by repeated measures separated by 1 week. For spatial normalization, high-resolution T2-weighted images were obtained using a RARE sequence with the following parameters: TR = 6 s, effective TE = 37.47 ms, RARE factor = 8, average number = 12, FOV = 30 × 30 mm^2, matrix size = 200 × 200, spatial resolution = 0.15 × 0.15 mm^2, the number of slices = 50 axial slices, no gap between slices, and slice thickness = 0.3 mm. Total scanning time was 30 min.

fMRI Data Preprocessing

Resting-state data processing was performed using FSL software and custom scripts in MATLAB. Since our data were acquired at 7 T with a voxel size of 0.47 mm, our voxel size had to be increased by the factor 10 in each dimension to match human data and to ensure correct processing by FSL. Preprocessing of the runs included (1) slice time correction (interleaved acquisitions), (2) motion correction (using mcFLIRT [Jenkinson et al., 2002]), (3) removal of nonbrain structures (by applying a brain mask), (4) mean-based intensity normalization to a factor of 10,000 (for group analysis), and (5) removal of linear trends and band-pass filtering (0.01–0.25 Hz, using the REST toolbox [Song et al., 2011]). Note that in this study, resting-state data were filtered in a relatively wider frequency band compared to the common frequency

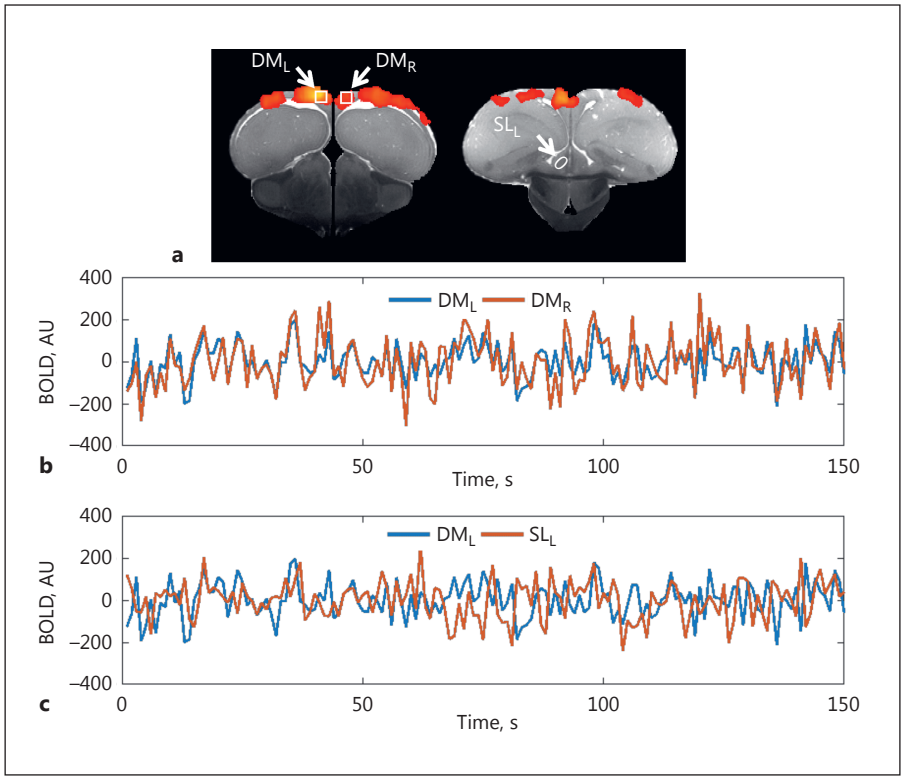

Fig. 1. Depiction of the functional connectivity analysis conducted in this study. **a** Selected brain regions are exemplarily shown. Frontal sections are from A6.50 (left) and A7.75 (right) from the pigeon brain atlas [Karten and Hodos, 1967]. Seeds for the BOLD fluctuation analysis depicted in **b** are from left (DM_L) and right dorsomedial region (DM_R) which are highlighted with a square. **b** Intrinsic BOLD fluctuations averaged from the DM region of both left and right hemispheres in one pigeon over 5 min (of 10 min total scan time). As visible, these two signals are highly correlated over time ($r = 0.78$). **c** BOLD fluctuations with low correlation ($r = 0.08$) averaged from the DM_L and left lateral septum region (SL_L). AU, arbitrary units.

used in human rs-fMRI data processing (0.01–0.1 Hz), since the majority of power in the pigeon resting-state data was observed in a wider range than the usual 0.01–0.1 Hz. The preprocessed data were first co-registered to the individual's high-resolution T2-weighted structural images, which was subsequently normalized to the low-resolution version of the pigeon MR atlas (3 × 3 × 3 mm) [Güntürkün et al., 2013] using affine linear registration (12 degrees of freedom) [Jenkinson et al., 2002]. The preprocessed functional data were spatially smoothed using 3D gaussian filtering (imgaussfilt3 function in MATLAB) with sigma = 0.5 after rescaling.

Region of Interest Analysis

Seed-based correlations were used to investigate the different patterns of functional connectivity of the regions of interest (ROIs) in both left and right hemispheres based on the pigeon brain MRI atlas [Güntürkün et al., 2013] and the map of Herold et al. [2014]. The reference time course for each ROI was created by averaging the time course of all voxels in the central part of each subdivision within the individual subject with a distance of at least 6 mm between the ROIs after rescaling. To be conservative, we used small sigma during spatial smoothing to avoid mixing information between selected ROIs.

Functional Connectivity

Functional connectivity was evaluated by multiple regression analyses carried out for each animal using the FEAT function of FSL. A separate regression model was created for each seed which included seed time course as an explanatory variable and seven nuisance covariates as explanatory variable confounders. The nuisance covariates were time series of global signals and six motion parameters. Single subject maps were used in the group level analysis which was carried out in the mixed-effect model of FSL (FLAME1). Correction for multiple comparisons was carried out at the cluster level using gaussian random field theory ($z > 2.3$; cluster significance: $p < 0.05$). To test whether the parametric statistical method for cluster-wise inference as implemented in FSL produced an overestimation of the functional connectivity pattern [Eklund et al., 2016], we conducted a group level analysis using threshold-free cluster enhancement [Smith and Nichols, 2009]. Family-wise errors were corrected at $p < 0.05$. The results were highly similar to those found with parametric cluster-wise inference. We therefore only depict the parametric results.

The functional connectivity matrix in Figure 3a was based on the number of activated voxels within ROIs. For instance, if the seed region was left Tr, the number of correlated voxels within each selected ROI was counted and normalized to the number of all voxels within the respective ROI. It is important to note that the values in Figure 3a are not correlation coefficients but percentages of voxels in an anatomical region that significantly covary in time with the seed region. Here is an example: If the value in, say, left DL after seeding in left DM is 0.86, this implies that 86% of left DL voxels evinced BOLD fluctuations that were significantly correlated with the BOLD fluctuations in the seed area of left DM. This then would imply a strong covariance of many left DL neurons with the activity pattern in left DM and would be interpreted as a high functional connectivity. If the connection pattern would not be 0.86 but, say, 0.01, such a covariance would only be true for 1% of the voxels. This, however, would not imply that this 1% of voxels are not significantly correlated. In fact, they are, but their number is small in this region. Figure 3b depicts the graphical summary of these analyses.

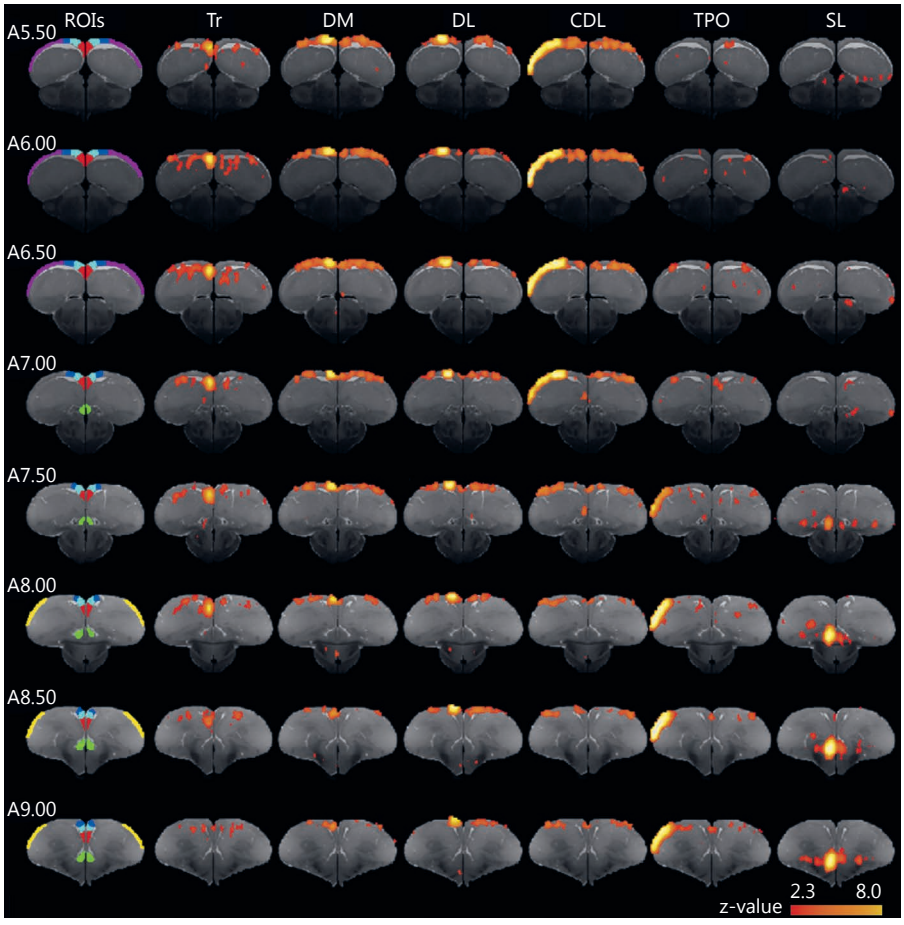

Fig. 2. Functional connectivity map of the left hemispheric hippocampal network. The column on the left shows the localization of the regions of interest depicted in frontal view: red, triangular region (Tr); cyan, dorsomedial region (DM); blue, dorsolateral region (DL); purple, dorsolateral corticoid area (CDL); yellow, area temporo-parieto-occipitalis (TPO); green, lateral septum (SL). The remaining columns show positive correlations of BOLD signals in areas of the telencephalon after seeding one of these regions in the left hemisphere (from left to right Tr, DM, DL, CDL, TPO, and SL). Negative correlations and data from seeding of right hemispheric regions are not shown. The color code represents the significance level for positive correlations of the selected region of interest (ROI) with a threshold at $z \geq 2.3$ ($p \leq 0.05$).

Results

This study presents an analysis of the correlation of BOLD fluctuations during rs-fMRI in six areas of the hippocampal network and its closely associated structures: DL, DM, and TR, CDL, TPO, and SL. Examples of significant and insignificant BOLD signal correlations are shown in Figure 1. Figure 1b depicts a high BOLD signal correlation of $r = 0.78$ ($p < 10^{-9}$) over a time course of 5 min between left and right DM. Figure 1c shows a very low and nonsignificant correlation of $r = 0.08$ between left DM and left SL.

Functional Connectivity Pattern of the Hippocampal Network

Triangular Region. Tr evinced a high number of positively correlated voxels with the DM over most of its whole anterior/posterior extent (seed in left Tr = 0.6; seed in right Tr = 0.48) (Fig. 2, 3a). Higher values were found for the left hemisphere, but on average about half of the voxels in DM of both hemispheres fluctuated in time with the changes of activity in their ipsilateral Tr. These correlations were mainly limited to the ventromedial DM portions, with no correlations present for the regions most adjacent to DL (Fig. 2). Contralateral connectivity between Tr and DM was considerably lower. Except for a few patchy voxels, functional connectivity measures with other structures of the analyzed network were close to zero (Fig. 2).

Dorsomedial Region. Activity fluctuations of both the left and the right DM were highly correlated with the whole DL (seed in left DM = 0.86; seed in right DM = 0.87). Prominent but smaller correlations were found for ipsilateral connections to CDL, especially its dorsomedial component, as well in the dorsal parts of posterior Tr. Connections to TPO and especially SL were low to absent. Right and left DM did not differ much in their functional connectivity patterns (Fig. 2, 3).

Dorsolateral Region. The correlation map generated by left and right DL seeds revealed positive ipsilateral correlations with the DM (seed in left DL = 0.47; seed in right

DL = 0.44). Thus, about half of DM voxels altered their activity patterns in time with the DL. The connectional value for ipsilateral CDL was only 0.23 (left) and 0.25 (right) with the majority of significantly correlated voxels being found adjacent to DL. The percentage of correlated voxels for Tr, TPO, and SL was very low.

Area Corticoidea Dorsolateralis. Resting-state activity of both left and right CDL were significantly and positively correlated with about 2/3 of the voxels in ipsilateral DL and DM. Interestingly, about the same connectional strength was observed for contralateral DL and DM. Connectional strengths to Tr and TPO were lower (between 0.14 and 0.29). Again, the connection of left CDL with left Tr was higher than for the same connection in the right hemisphere. No significantly correlated voxels were discovered in SL.

Area Temporo-Parieto-Occipitalis. Overall, only small numbers of voxels in the analyzed hippocampal network covaried with the activity patterns of the TPO. Connectional strengths of left (0.11) and right (0.18) TPO with left and right DM, respectively, were of quite modest strengths. The connectional strength of right TPO to the ipsilateral DL also reached only 0.11. All other connections were small or, in the case of SL, negligible (Fig. 2b, 3).

Septum Laterale. Seeding of SL evinced only few correlated voxels in DM and CDL (Fig. 2). In most cases, the percentage of significant voxels amounted to less than 0.01 of the voxel number of the regions under analysis and is not reported here. Due to these extremely small numbers of correlated voxels within the hippocampal network after SL seeding, Figure 3 shows SL without a functional connection to the rest of the system (Fig. 3).

Homotopic Bilateral Connectivity. We discovered strong homotopic, but mostly weaker heterotopic, connectivities between hemispheres. The strongest connectivities of DM, DL, and Tr existed with their respective contralateral counterparts (DM: left seed = 0.74; right seed = 0.67; DL: left seed = 0.65; right seed = 0.76; Tr: left seed = 0.44; right seed = 0.56). This does not apply to TPO (left seed = 0.12; right seed = 0.02). SL did not show functional connections to the hippocampal network but is tightly functionally linked to its homotopic counterpart (left seed = 0.64; right seed = 0.74).

Discussion

The current study is the first functional connectivity analysis on the different components of the avian hippocampal network. A previous study had already analyzed the functional and asymmetrically organized connectivity patterns of the overall hippocampal system [Jonckers et al., 2015]. The current study thus complements the diverse structural [Erichsen et al., 1991; Tömböl et al., 2000b; Herold et al., 2014; Striedter, 2016], tracing-based connectional [Tömböl et al., 2000b; Kahn et al., 2003; Atoji and Wild, 2004, 2005; Atoji et al., 2016], and physiological studies [Hough et al., 2002; Siegel et al., 2005] that mapped the bird hippocampus along with its internal connections. A resting-state functional connectivity analysis delivers different result patterns than a tracing study: Structures that are monosynaptically connected can still show very low functional connectivity under rest, when these two structures only couple during specific task components. We will discuss this for the SL. In addition, a high degree of functional connectivity does not necessarily imply a direct anatomical link, since areas that are only indirectly connected via a third structure can still be tightly functionally coupled. This is discussed below for the functional connection of CDL and DL. Thus, an imaging-based connectivity analysis reveals functional couplings within a neural system and so uncovers a structurally otherwise invisible architecture of a whole network. This approach, therefore, visualizes the dynamic blueprints of a system and constitutes a complement to structural connectivity analyses. We will now discuss our findings, one by one, starting with CDL.

Area Corticoidea Dorsolateralis

Atoji and Wild [2005] extensively analyzed the fiber connections of the CDL and demonstrated that it could serve as a gateway to the avian hippocampal system through its reciprocal connections with visual thalamofugal, olfactory, and limbic structures, including the medial and lateral septum [Atoji and Wild, 2005; Patzke et al., 2011]. In addition, CDL can modulate the motor output via its connections to the striatum [Kröner and Güntürkün, 1999]. Within the hippocampal system, CDL has reciprocal projections with lateral DM and Tr [Atoji and Wild, 2005]. Connections with DL were reported to be very weak. Our analysis shows that these findings do not fully translate into the realm of functional connectivity. While indeed CDL activity patterns correlate with those of DM, the BOLD signal of CDL also covaries strongly with DL, but it correlates only very weakly with Tr. It is possible that DM serves as a central hub and thus transfers a common pace between CDL and DL, although these two areas are only weakly connected at the structural level.

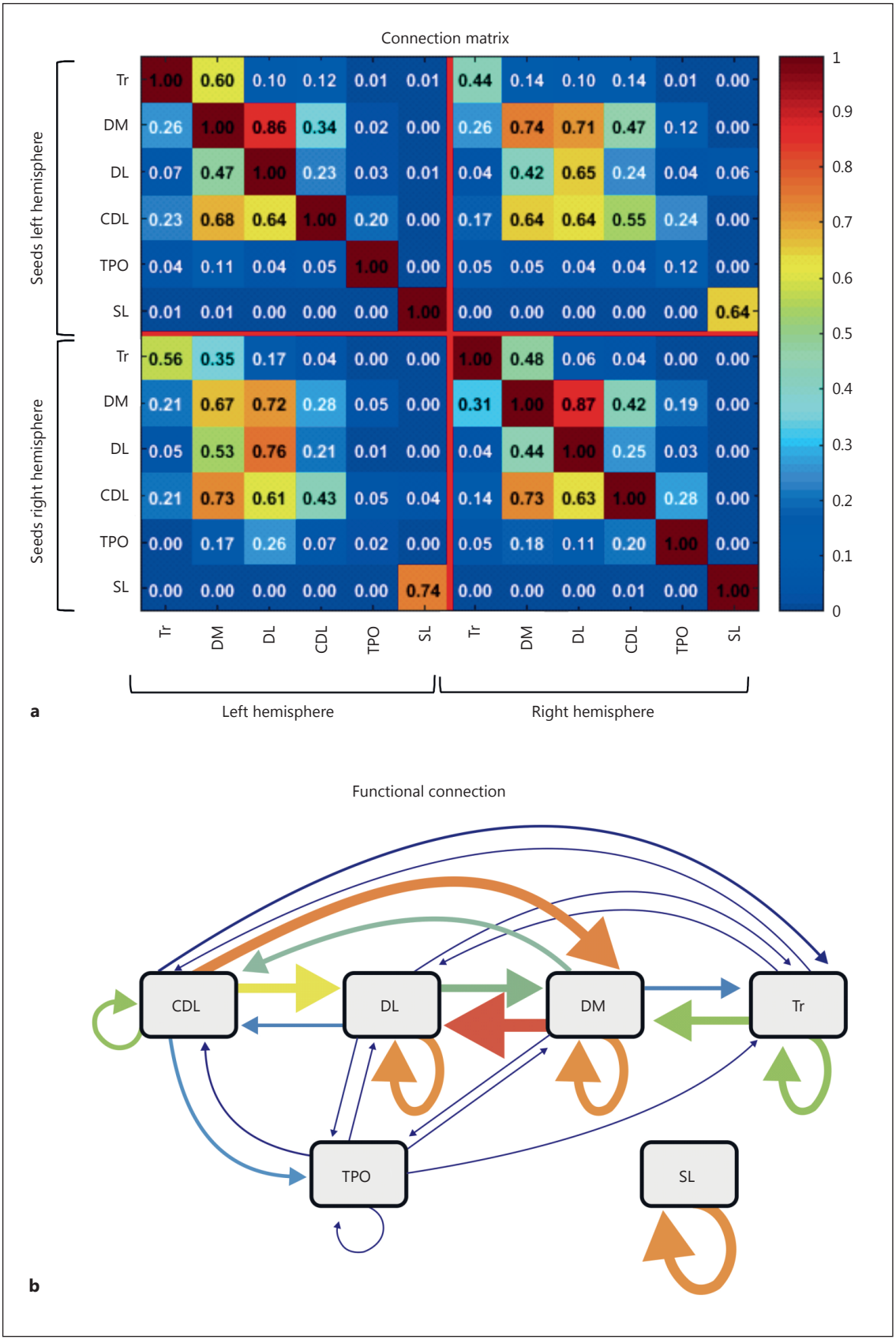

3

(For legend see next page.)

Brain Behav Evol 2017;90:62–72
DOI: 10.1159/000475591

Dorsolateral Region

Several authors reported a strong structural and physiological reciprocal link between DL and DM [Hough et al., 2002; Siegel et al., 2002; Kahn et al., 2003; Atoji and Wild, 2004]. Our results fully support these data and show that DL voxels strongly correlate with the DM BOLD fluctuations. Tract tracing data show that in addition to its intrahippocampal connections, DL is also reciprocally connected to various thalamofugal visual regions as well to the nidopallial convergence zone of the visual thalamo- and tectofugal systems [Casini et al., 1986; Shimizu et al., 1995; Husband and Shimizu, 1999; Atoji and Wild, 2004; Shanahan et al., 2013]. DL also receives olfactory information [Bingman et al., 1994] and limbic input [Cheng et al., 1999]. Since information from various senses are funneled via DL into the hippocampal formation, many authors proposed that DL might correspond to the mammalian entorhinal cortex [Kahn et al., 2003; Atoji and Wild, 2004; Rattenborg and Martinez-Gonzalez, 2011]. Our functional connectivity data show that DL is indeed ideally suited to take a role similar to the entorhinal cortex due to its dense connections with CDL, DM, and, via DM, the Tr. It thus communicates closely with the core constituents of the avian hippocampal system.

Dorsomedial Region

Our data suggest that DM is the central hub within the avian hippocampal system. It is strongly connected to DL and CDL and so couples these two structures that are anatomically only weakly linked. As a result, DM could play the role of a gatekeeper for sensory information that enters the hippocampus via CDL and DL. DM is also the only structure with which Tr has strong connections. These functional connectivity data nicely match the results from tracing studies [Kahn et al., 2003; Atoji and Wild, 2004]. According to Atoji et al. [2016], DM neurons project to SL while Tr neurons do not. Based on these and further findings, they propose that DM corresponds to Ammon's horn since pyramidal neurons of this structure are known to project to the lateral septum [Strange et al., 2014]. There are, however, also proposals that are based on physiological and other connectional data and that assume that Tr, or more precisely, the medial and lateral layer of Tr correspond to Ammon's horn [Siegel et al., 2002; Kahn et al., 2003]. Herold et al. [2014] revealed that both DM and Tr overlap with respect to their neurochemical profile with Ammon's horn. The present study shows that neither DM nor Tr are functionally linked to SL. As discussed below, this does neither contradict the proposed homologies nor the tracing data. It shows, however, that tightly structurally connected structures can stay functionally disconnected for extensive periods of resting time. We will discuss this below.

Triangular Region

According to various anatomical studies, the Tr of the avian hippocampus can be subdivided into two narrow wings that encapsulate a triangular part [Kahn et al., 2003; Atoji and Wild, 2004; Herold et al., 2014]. We fused these areas into a single ROI due to resolution limitations of the MRI approach. Tract tracing studies show that Tr is reciprocally connected to DL and DM [Atoji et al., 2002; Kahn et al., 2003; Atoji and Wild, 2004]. The V-shaped layer of Tr stains for Prox1 mRNA, a gene marker for the mammalian dentate gyrus [Atoji et al., 2016]. Based on this finding and the observation that Tr hardly projects to SL, these authors argue that the wing-shaped parts of Tr could constitute the avian dentate gyrus [but see Kahn et al., 2003].

Fig. 3. Quantitative (**a**) and graphical (**b**) depiction of the resting-state functional connectivity data. **a** Functional connectivity matrix of all analyzed structures in the left and the right hemisphere. Numbers give the proportion of voxels that were significantly correlated after seeding. Seeded areas are shown on the *y*-axis; the *x*-axis depicts the structure that was analyzed with respect to the percentage of voxels that were significantly correlated with the seed. For example, when the left DM is seeded, 26% of the voxels in left Tr are significantly correlated with the BOLD fluctuation in left DL (please look up the box on the leftmost column, second from top). The light blue color code in this box indicates the percentage of significantly activated voxels and can be matched with the heat map on the right side. **b** Graphical depiction of these data, based on an average of the left and the right hemisphere. The size and the color of the arrows match the strength of functional connectivity. The color code is identical to that of **a** and wider arrows depict stronger connections. Curved arrows show connectional strength with the homotopic area of the other hemisphere. Otherwise only ipsilateral connections are depicted. Connectional strengths of 1% or less are not shown; therefore, SL seems not to be connected to the remaining system, with the exception to its strong coupling to the SL of the other hemisphere. The direction of arrows shows seeding direction. If structure A is seeded and structure B is analyzed with respect to the percentage of voxels that correlate with their activity fluctuations with the seed in structure A, then the arrow points from A to B. See legend to Figure 2 for abbreviations.

Our functional connectivity data show that Tr is strongly connected to DM, while the functional connections to other areas of the hippocampal networks are very weak. Indeed, Atoji and Wild [2004] described that Tr receives afferents from DL and DM but in turn mainly projects back upon DM. Indeed, we could show that more than half of DM voxels were significantly correlated with BOLD signal fluctuations in Tr. Thus, slow activity fluctuations in Tr are only minimally influenced by DL input but are in pace with activity changes in DM.

In pigeons, the left hippocampus plays a key role in navigational map and sun compass-based learning as well as in the encoding of goal locations based on environmental geometry [Gagliardo et al., 2001, 2005; Nardi and Bingman, 2007]. Consequently, pigeons display right-eye superiority during homing [Ulrich et al., 1999; Prior et al., 2004]. Jonckers et al. [2015] demonstrated in an rs-fMRI analysis that left-sided hippocampal seeding in pigeons consistently resulted in larger functional connectivity maps than right-sided ones. Unfortunately, the seeds in the study by Jonckers et al. [2015] were often encompassing more than one hippocampal subregion, although it involved mostly Tr. Indeed, our study shows that left Tr evinced a higher number of positively correlated voxels with DM and CDL than right Tr. This could imply, that asymmetries of functional Tr connectivity could play a key role for left-right differences of hippocampal functions like navigational control [Mouritsen et al., 2016].

Area Temporo-Parieto-Occipitalis

TPO communicates with the hippocampal network mainly via CDL. Different from CDL, TPO has limited afferents from limbic structures but connects to visual areas of the thalamofugal and the tectofugal system [Husband and Shimizu, 1999; Atoji and Wild, 2005]. Importantly, TPO also participates in the descending tractus septomesencephalicus and thus projects to a large number of subtelencephalic structures like the optic tectum [Manns et al., 2007; Stacho et al., 2016]. Via its terminations in the deep tectal layers, TPO could potentially play a role for motor output.

Septum Laterale

Seeding SL did not reveal correlated activity to any of the core regions of the hippocampal formation. Although there were correlations to few Tr and DM voxels, these correlations never exceeded 1% of the voxel space (Fig. 3). This finding is of high relevance since a recent study by Atoji et al. [2016] found that glutamatergic neurons of DM project to SL, a characteristic which is shared by glutamatergic neurons in the mammalian Ammon's horn. In mammals, the septum projects back to the hippocampus and drives hippocampal theta rhythms, which are essential for learning and memory functions [Winson, 1978; Leutgeb and Mizumori, 1999; Vandecasteele et al., 2014; Robinson et al., 2016]. The lack of functional connectivity between SL and the analyzed hippocampal regions could indicate an important functional difference of SL in the avian hippocampal network. However, a recent study applying rs-fMRI in rats found that a functional connectivity between hippocampus (CA3 and dentate gyrus) and septum only became visible when the animals had learned a task prior to scanning [Nasrallah et al., 2016]. This could also be the case in pigeons, which calls for similar future rs-fMRI experiments on the avian hippocampal network in birds.

Concluding Remarks

Our rs-fMRI analysis reveals that the arrangement of reciprocal connectivities between CDL, DL, DM, and Tr is the functional backbone of the pigeon hippocampal system. At least under resting state, TPO and SL are far less coupled to this network (Fig. 3b). Both CDL and DL could serve as input and output structures. Our results show that DM, by its strong connections to both DL and CDL, is clearly the central hub of the hippocampal system and could control sensory information flow into the hippocampus via these two structures. In addition, DM is the only structure with which Tr has strong functional connections. Thus, activity patterns of Tr are importantly coupled to DM but are only weakly modulated by other areas of the hippocampal network. In addition, we discovered strong interhemispheric connections between homotopic hippocampal areas. The avian hippocampus plays a key role for navigation during flight by utilizing multiple map-like, spatial representations of landmarks and compass information that reside in a distributed manner in the different associative sensory areas of both hemispheres [Mouritsen et al., 2016]. Integrating this information between hemispheres to compute navigational routes could be the essential function of these interhemispheric connections.

Acknowledgments

O.G. was supported by the German Research Foundation (DFG or Deutsche Forschungsgemeinschaft) through SFB 874. Animal imaging was conducted at the Ruhr University Bochum Imaging Center with support from the Mercator Foundation.

References

Atoji Y, Sarkar S, Wild JM (2016): Proposed homology of the dorsomedial subdivision and V-shaped layer of the avian hippocampus to Ammon's horn and dentate gyrus, respectively. Hippocampus 26:1608–1617.

Atoji Y, Wild JM (2004): Fiber connections of the hippocampal formation and septum and subdivisions of the hippocampal formation in the pigeon as revealed by tract tracing and kainic acid lesions. J Comp Neurol 475:426–461.

Atoji Y, Wild JM (2005): Afferent and efferent connections of the dorsolateral corticoid area and a comparison with connections of the temporo-parieto-occipital area in the pigeon (*Columba livia*). J Comp Neurol 485:165–182.

Atoji Y, Wild JM (2014): Efferent and afferent connections of the olfactory bulb and prepiriform cortex in the pigeon (*Columba livia*). J Comp Neurol 522:1728–1752.

Atoji Y, Wild JM, Yamamoto Y, Suzuki Y (2002): Intratelencephalic connections of the hippocampus in pigeons (*Columba livia*). J Comp Neurol 447:177–199.

Bingman VP, Casini G, Nocjar C, Jones TJ (1994): Connections of the piriform cortex in homing pigeons *(Columba livia)* studied with fast blue and WGA-HRP. Brain Behav Evol 43:206–218.

Bingman VP, Gagliardo A, Hough GE, Ioalé P, Kahn MC, Siegel JJ (2005): The avian hippocampus, homing in pigeons and the memory representation of large-scale space. Integr Comp Biol 45:555–564.

Bingman VP, Salas C, Rodriguez F: Evolution of the hippocampus (2009): in Binder MD, Hirokawa N, Windhorst U (eds): Encyclopedia of Neuroscience. Berlin, Springer, pp 1356–1360.

Casini G, Bingman VP, Bagnoli P (1986): Connections of the pigeon dorsomedial forebrain studied with WGA-HRP and ^{3}H-proline. J Comp Neurol 245:454–470.

Cheng M, Chaiken M, Zuo M, Miller H (1999): Nucleus taenia of the amygdala of birds: anatomical and functional studies in ring doves (*Streptopelia risoria*) and European starlings (*Sturnus vulgaris*). Brain Behav Evol 53:243–270.

Daliri MR, Behroozi M (2014): Advantages and disadvantages of resting state functional connectivity magnetic resonance imaging for clinical applications. OMICS J Radiology 3:e123.

De Groof G, Jonckers E, Güntürkün O, Denolf P, Van Auderkerke J, Van der Linden A (2013): Functional MRI and functional connectivity of the visual system of awake pigeons. Behav Brain Res 239:43–50.

Di Martino A, Scheres A, Margulies DS, Kelly AMC, Uddin LQ, Shehzad Z, Biswal B, Walters JR, Castellanos FX, Milham MP (2008): Functional connectivity of human striatum: a resting state FMRI study. Cereb Cortex 18: 2735–2747.

Eklund A, Nichols TE, Knutsson H (2016): Cluster failure: why fMRI inferences for spatial extent have inflated false-positive rates. Proc Natl Acad Sci USA 113:7900–7905.

Erichsen JT, Bingman VP, Krebs JR (1991): The distribution of neuropeptides in the dorsomedial telencephalon of the pigeon (*Columba livia*): a basis for regional subdivisions. J Comp Neurol 314:478–492.

Fox MD, Raichle ME (2007): Spontaneous fluctuations in brain activity observed with functional magnetic resonance imaging. Nat Rev Neurosci 8:700–711.

Gagliardo A, Ioalè P, Odetti F, Bingman VP, Siegel JJ, Vallortigara G (2001): Hippocampus and homing in pigeons: left and right hemispheric differences in navigational map learning. Eur J Neurosci 13:1617–1624.

Gagliardo A, Vallortigara G, Nardi D, Bingman VP (2005): A lateralized avian hippocampus: preferential role of the left hippocampal formation in homing pigeon sun compass-based spatial learning. Eur J Neurosci 22:2549–2559.

Güntürkün O, Verhoye M, De Groof G, Van der Linden A (2013): A 3-dimensional digital atlas of the ascending sensory and the descending motor systems in the pigeon brain. Brain Struct Funct 218:269–281.

Herold C, Bingman VP, Ströckens F, Letzner S, Sauvage M, Palomero-Gallagher N, Zilles K, Güntürkün O (2014): Distribution of neurotransmitter receptors and zinc in the pigeon (*Columba livia*) hippocampal formation: a basis for further comparison with the mammalian hippocampus. J Comp Neurol 522: 2553–2575.

Herold C, Coppola VJ, Bingman VP (2015): The maturation of research into the avian hippocampal formation: recent discoveries from one of the nature's foremost navigators. Hippocampus 25:1193–1211.

Hough GE, Pang KCH, Bingman VP (2002): Intrahippocampal connections in the pigeon (*Columba livia*) as revealed by stimulation evoked field potentials. J Comp Neurol 452: 297–309.

Hurwitz R, Lane SR, Bell RA, Brant-Zawadzki MN (1989): Acoustic analysis of gradient-coil noise in MR imaging. Radiology 173:545–548.

Husband SA, Shimizu T (1999): Efferent projections of the ectostriatum in the pigeon (*Columba livia*). J Comp Neurol 406:329–345.

Jenkinson M, Bannister P, Brady M, Smith S (2002): Improved optimization for the robust and accurate linear registration and motion correction of brain images. NeuroImage 17: 825–841.

Jonckers E, Güntürkün O, De Groof G, Van der Linden A, Bingman VP (2015): Network structure of functional hippocampal lateralization in birds. Hippocampus 25:1418–1428.

Kahn MC, Hough GE, Ten Eyck GR, Bingman VP (2003): Internal connectivity of the homing pigeon (*Columba livia*) hippocampal formation: an anterograde and retrograde tracer study. J Comp Neurol 459:127–141.

Kaplan R, Adhikari MH, Hindriks R, Mantini D, Murayama Y, Logothetis NK, Deco G (2016): Hippocampal sharp-wave ripples influence selective activation of the default mode network. Curr Biol 26:686–691.

Karten HJ, Hodos W (1967): Stereotaxic atlas of the brain of the pigeon (*Columba livia*). Baltimore, Johns Hopkins University Press.

Kröner S, Güntürkün O (1999): Afferent and efferent connections of the caudolateral neostriatum in the pigeon (*Columba livia*): a retro- and anterograde pathway tracing study. J Comp Neurol 407:228–260.

Leutgeb S, Mizumori SJ (1999): Excitotoxic septal lesions result in spatial memory deficits and altered flexibility of hippocampal single-unit representations. J Neurosci 19:6661–6672.

Logothetis NK, Pauls J, Augath M, Trinath T, Oeltermann A (2001): Neurophysiological investigation of the basis of the fMRI signal. Nature 412:150–157.

Manns M, Freund N, Patzke N, Güntürkün O (2007): Organization of telencephalotectal projections in pigeons: impact for lateralized top-down control. Neuroscience 144:645–653.

Mouritsen H, Heyers D, Güntürkün O (2016): The neural basis of long-distance navigation in birds. Annu Rev Physiol 78:133–154.

Nardi D, Bingman VP (2007): Asymmetrical participation of the left and right hippocampus for representing environmental geometry in homing pigeons. Behav Brain Res 178:160–171.

Nasrallah FA, To XV, Chen D-Y, Routtenberg A, Chuang K-H (2016): Functional connectivity MRI tracks memory networks after maze learning in rodents. NeuroImage 127:196–202.

Patzke N, Manns M, Güntürkün O (2011): Telencephalic organization of the olfactory system in homing pigeons (*Columba livia*). Neuroscience 194:53–61.

Prior H, Wiltschko R, Stapput K, Güntürkün O, Wiltschko W (2004): Visual lateralization and homing in pigeons. Behav Brain Res 154:301–310.

Rattenborg NC, Martinez-Gonzalez D (2011): A bird-brain view of episodic memory. Behav Brain Res 222:236–245.

Robinson J, Manseau F, Ducharme G, Amilhon B, Vigneault E, Mestikawy SE, Williams S (2016): Optogenetic activation of septal glutamatergic neurons drive hippocampal theta rhythms. J Neurosci 36:3016–3023.

Shanahan M, Bingman VP, Shimizu T, Wild M, Güntürkün O (2013): Large-scale network organization in the avian forebrain: a connectivity matrix and theoretical analysis. Front Comput Neurosci 7:89.

Shimizu T, Cox K, Karten HJ (1995): Intratelencephalic projections of the visual wulst in pigeons (*Columba livia*). J Comp Neurol 359: 551–572.

Siegel JJ, Nitz D, Bingman VP (2002): Electrophysiological profile of avian hippocampal unit activity: a basis for regional subdivisions. J Comp Neurol 445:256–268.

Siegel JJ, Nitz D, Bingman VP (2005): Spatial-specificity of single-units in the hippocampal formation of freely moving homing pigeons. Hippocampus 15:26–40.

Smith SM, Nichols TE (2009): Threshold-free cluster enhancement: addressing problems of smoothing, threshold dependence and localisation in cluster inference. NeuroImage 44: 83–98.

Smulders TV (2017) The avian hippocampal formation and the stress response. Brain Behav Evol 90:81–91.

Song X-W, Dong Z-Y, Long X-Y, Li S-F, Zuo XN, Zhu CZ, He Y, Yan CG, Zang YF (2011): REST: a toolkit for resting-state functional magnetic resonance imaging data processing. PLoS One 6:e25031.

Stacho M, Letzner S, Theiss C, Manns M, Güntürkün O (2016): A GABAergic tectotegmento-tectal pathway in pigeons. J Comp Neurol 524:2886–2913.

Strange BA, Witter MP, Lein ES, Moser EI (2014): Functional organization of the hippocampal longitudinal axis. Nat Rev Neurosci 15:655–669.

Striedter GF (2016): Evolution of the hippocampus in reptiles and birds. J Comp Neurol 524: 496–517.

Tömböl T, Davies DC, Németh A, Sebestény T, Alpár A (2000a): A comparative Golgi study of chicken (*Gallus domesticus*) and homing pigeon (*Columba livia*) hippocampus. Anat Embryol (Berl) 201:85–101.

Tömböl T, Davies DC, Németh A, Alpár A, Sebestény T (2000b): A Golgi and a combined Golgi/GABA immunogold study of local circuit neurons in the homing pigeon hippocampus. Anat Embryol (Berl) 201:181–196.

Treves A, Tashiro A, Witter MP, Moser EI (2008): What is the mammalian dentate gyrus good for? Neuroscience 154:1155–1172.

Ulrich C, Prior H, Duka T, Leshchins'ka I, Valenti P, Güntürkün O, Lipp HP (1999): Left-hemispheric superiority for visuospatial orientation in homing pigeons. Behav Brain Res 104:169–178.

Vandecasteele M, Varga V, Berényi A, Papp E, Barthó P, Venance L, Freund TF, Buzsáki G (2014): Optogenetic activation of septal cholinergic neurons suppresses sharp wave ripples and enhances theta oscillations in the hippocampus. Proc Natl Acad Sci USA 111: 13535–13540.

van den Heuvel MP, Hulshoff Pol HE (2010): Exploring the brain network: a review on resting-state fMRI functional connectivity. Eur Neuropsychopharmacol 20:519–534.

Winson J (1978): Loss of hippocampal theta rhythm results in spatial memory deficit in the rat. Science 201:160–163.